

Performance Analysis and MPPT Control of a Standalone Hybrid Power Generation System

G. Ganesh*, G Vijay Kumar

Department of Electrical and Electronics Engineering, SC College of Engineering, Kharimnagar, India.

*ganeshgowri@hotmail.com

A.R. Vijay Babu, G. Srinivasa Rao, Y.R.Tagore

School of Electrical Engineering, Vignana's University, Guntur, India.

Abstract--In this paper, a standalone Hybrid power generation system with improved power quality is proposed. The proposed system consisting of Wind energy conversion system (WECS), Diesel generator system, PV generation system and Battery energy storage system (BESS). A hybrid system consists of wind, solar PV, diesel generator, battery, and a controller. Tip Speed Ratio (TSR) control with Field Oriented Control (FOC), method was used for implementing Maximum Power Point Tracking (MPPT) for wind system, variable step Perturb & Observing (P&O) method for solar and optimum fuel consumption technique for Diesel engine. MATLAB/Simulink was used to build the model and simulate the system. The result shows the better performance of the system under the variation of input constraints as well as output constraints.

Index Terms— Hybrid Power Generation, Maximum Power Point Tracking (MPPT), Field Oriented Control (FOC), Variable-step Perturb & Observing (P&O) Method, Battery energy storage system (BESS)

I. INTRODUCTION

Environmental concerns about global warming, fossil fuel exhaustion and the need to reduce carbon dioxide emissions provide the stimulus to seek renewable energy sources. Hybrid power systems, which combine conventional and renewable power conversion systems, are the best solution for feeding the mini-grids and isolated loads in remote areas. Properly chosen renewable power sources will considerably reduce the need for fossil fuel leading to an increase in the sustainability of the power supply. At the same time, conventional power sources aid the renewable sources in hard environmental conditions, which improve the reliability of the electrical system. Which is expected to: satisfy the load demands, minimize the costs, maximize the utilization of renewable sources, optimize the operation of battery bank, which is used as back up unit, ensure efficient operation of the diesel generator, and reduce the environment pollution emissions from diesel generator if it is used as a stand-alone power supply.

Nowadays, the growth of wind and PV power generation systems has exceeded the most optimistic estimation. In this paper, a stand-alone hybrid energy system consisting of wind, PV and diesel is proposed with the battery for energy storage. Wind and PV are the primary power sources of the system to take full advantages of renewable energy, and the diesel is used as a backup system. The dynamic modelling and control of the system is studied. The concept and principle of the

hybrid system with its supervisory control were delineated. Classical techniques of maximum power tracking were applied to PV array and the wind-turbine control in order to reduce complexity and cost.

In the wind generation system, the squirrel cage induction generator is introduced because it is robust and has low cost. Power generation using wind energy is possible in two ways, viz. constant speed operation and variable speed operation using power electronic converters. Variable speed power generation for a wind turbine is attractive; because maximum efficiency can be achieved at all wind velocities. The chosen variable speed WEG system consists of a wind turbine, squirrel-cage induction generator, an AC-DC-AC interface and the utility grid. In this paper the generator side converter is controlled using vector control of induction machine and the grid side converter is controlled using DC link voltage control. The vector control methods include a field-oriented controller (FOC) and direct torque controller (DTC) [1 13-15]. There are also other advanced controllers such as the sensor less controller [7] and the intelligent controllers [8]. However, these advanced controllers were developed to deal with special control problems, such as nonlinearity and machine parameter uncertainty. Their control mechanisms are the same as the FOC or DTC except the rotor speed estimation, and therefore will not be treated in this paper.

In some applications, the wind turbine may be augmented by an additional power source, usually a diesel generator. These systems are called wind-diesel systems [2] and may be used to supply electricity energy to stand-alone loads, e.g., small villages that are not connected to the main utility. Most diesel generation systems operate at a constant speed due to the restriction of constant frequency at the generator terminals. However, diesel engines have high fuel consumption when operating with light load and constant speed. In order to improve the efficiency and avoid wet stacking, a minimum load of about 30% to 40% is usually recommended by the manufacturers [3]. Variable-speed operation can increase the efficiency, where the fuel consumption can be reduced up to 40% [3], especially when operating with a light load. Moreover, the life expectancy can increase with a lower thermal signature. To avoid the frequent start/stop of the diesel energy storage system is often used.

$$P_m = \frac{1}{2} \rho A C_P(\lambda, \beta) V_\omega^3 \quad (2)$$

where ρ and A are the air density and the area swept by blades, respectively. V_ω is the wind velocity (m/s), and C_P is called the power coefficient, and is given as a nonlinear function of the tip speed ratio λ defined by

$$\lambda = \frac{\omega_r R}{V_\omega} \quad (3)$$

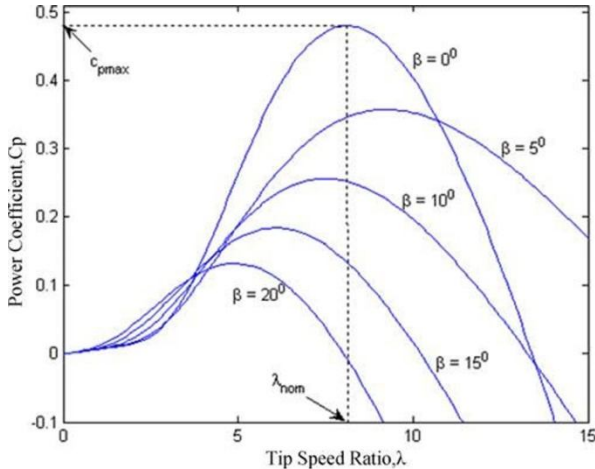
where R is the turbine blade radius, and ω_r is the turbine speed. C_P is a function of λ and the blade pitch angle β .

The variable-speed pitch-regulated wind turbine is considered in this paper, where the pitch angle controller plays an important role. Fig. 2 shows the groups of $C_P - \lambda$ at different pitch angles and speed- power curves of the wind turbine used in this study at different wind velocities. It is noted from the figure that C_P can be changed either by adjusting the pitch angle β or Tip speed ratio λ . Here considering constant pitch, In other words, the output power of the wind turbine can be regulated by the TSR control.

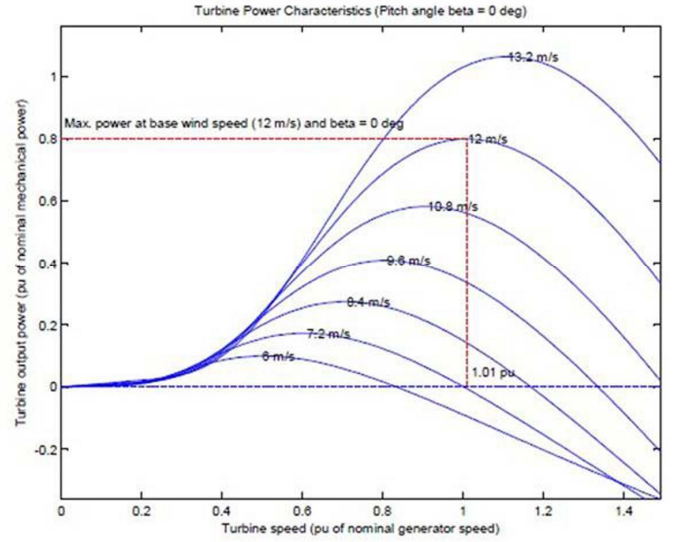
B. Diesel-Generator Set Model

The diesel-generator set (DGS) model is composed of combustion, drive train, and synchronous generator models. A common governor model is used in this paper; the essential features can be described by the transfer function described in [9].

The fuel consumption of a diesel engine depends on the speed and torque of the machine. Fig. 3 shows the fuel consumption curves of a diesel engine for various rotational speeds. It can be seen that at 20% rated power, there is a 50% fuel saving than that at 0.6 rated speed. According to Fig. 3, a continuous function for the optimal operation versus speeds can be formed tangent to all the curves. In order to minimize the fuel consumption, the speed demand (optimum speed) for the diesel engine is calculated by building up a look-up table where the optimal power-speed curve is implemented.



(a)



(b)

Fig.2(a) characteristics of the WECS at different pitch angles. (b) Turbine power characteristics (pitch angle $\beta = 0$ deg).

The excitation system used in diesel generator is Type-1 excitation model taken from IEEE Standard 421.5 [10].

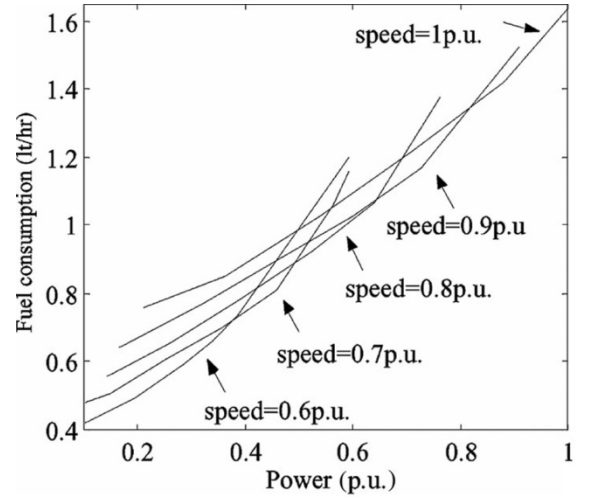


Fig.3 Fuel consumption versus power at various rotational speeds.

C. Photovoltaic Array Model

A solar cell is traditionally represented by an equivalent circuit composed of a current source, an anti-parallel diode, a series resistance and a shunt resistance. As shown in Fig. 4, the anti-parallel diode branch is modified to an external control current source which is anti-parallelled with the original current source [11].

$$I = I_{irr} - I_0 \left[\exp \left(q \cdot \frac{V + IR_S}{nkT} \right) - 1 \right] - \frac{V + IR_S}{R_P} \quad (4)$$

Where I_{irr} is the photo current or irradiance current, q is the electronic charge ($q = 1.602 \times 10^{-19}$ C), k is the Boltzmann constant ($k = 1.3806503 \times 10^{-23}$ J/K), n is the Ideality factor or

the ideal constant of the diode, T is the temperature of the cell, I_0 is the diode saturation current or cell reverse saturation current and $R_s R_p$ represent the series and shunt resistance, respectively.

$$I_{irr} = I_{irr,ref} \left(\frac{G}{G_{ref}} \right) \left[1 + \alpha'_T (T - T_{ref}) \right] \quad (5)$$

Where $I_{irr,ref}$ is the photo current at SRC. α'_T is the relative temperature coefficient of the short-circuit current, which represents the rate of change of the short-circuit current with respect to temperature

The output characteristics are drastically affected by the irradiation and temperature. Equations (4)–(5) show that the solar cell has nonlinear output characteristics. The P – V and I – V characteristics are shown in Fig. 5. When the output voltage change of solar array is small, the change of output current is extremely small and the solar array is considered as a constant current source. However, the current decreases quickly as the voltage exceed a critical value.

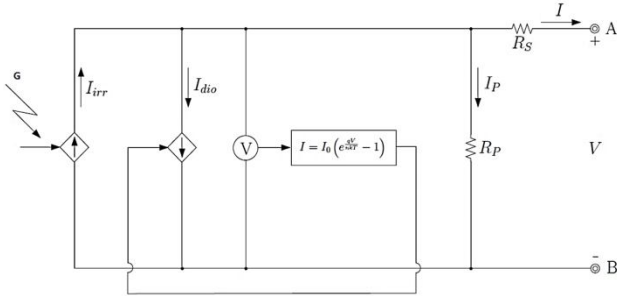


Fig.4 Modified equivalent circuit for a solar cell.

D. Battery Energy Storage System

The analyzed model of the battery storage system is obtained from a built-in template in MATLAB. The battery load current rapidly changes according to changes in weather conditions and power command for the bus inverter in operation. The dc-bus voltage must be regulated to stay within a stable region regardless of the battery-current variation. This was given in subsequent sections

III. MPPT CONTROL ALGORITHM OF THE PV SYSTEM

The most common method in this field is the P&O method [5]. It periodically increases or decreases the solar cell's voltage as mentioned before to seek the maximum power point. In this paper, a variable step method is proposed to search for the maximum power point, where the step length is adjusted according to the distances to the MPP. The ratio of the variation of power P to voltage V is considered as the step length of duty ratio D , which is actually the slope of each operating point under very short sampling time. Fig. 6 shows

the control block of the P&O method.

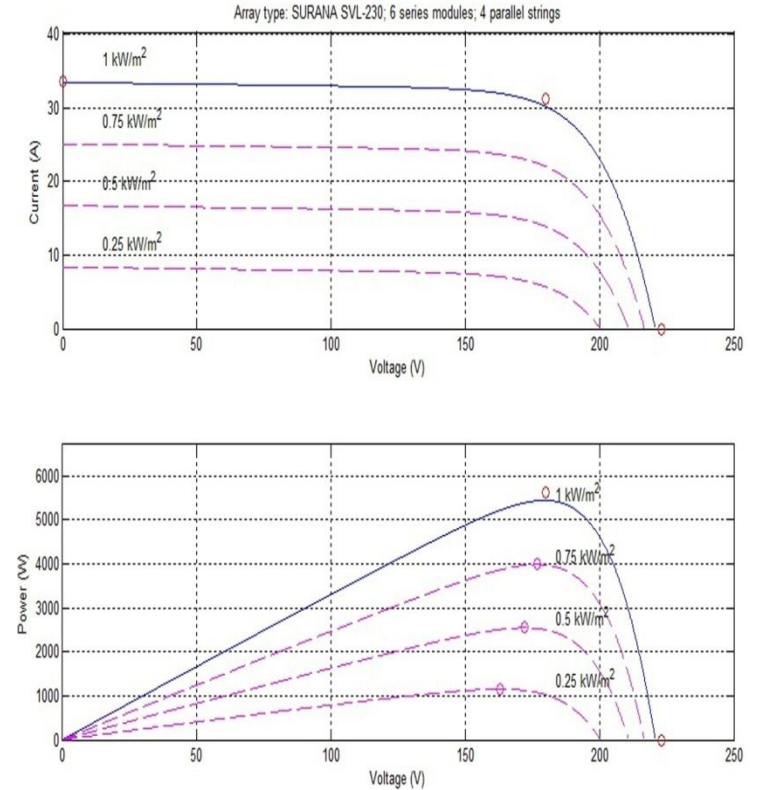


Fig.5 I-V and P-V characteristics of ARRAY (type: SURANA SVL-230, 6 series modules; 4 parallel strings) at 25deg.C

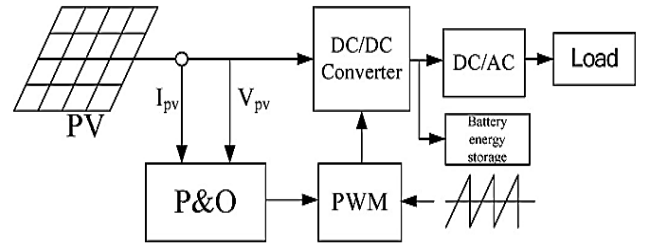
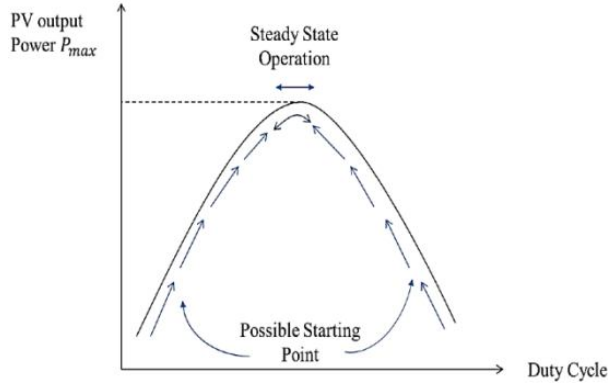
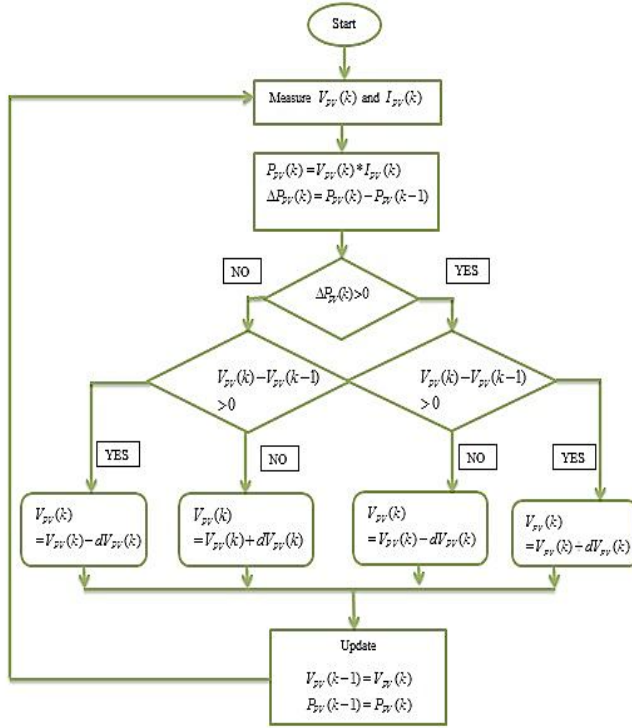


Fig.6 . Configuration of P&O Control System.

The principle of P&O MPPT strategy is to periodically vary next step direction by a fixed factor $\pm \Delta P_{PV} / \Delta V_{PV}$, which is considered as the perturbation cycle. As shown in figure 7(a), regardless of where the tracking point firstly starts, the final goal is to arrive at the steady state operation region around the maximum power point. by comparing the current PV array output power with that of the previous perturbation cycle. The flowchart of P&O algorithm is shown in Fig 7(b). The DC Bus Voltage regulation and VSC control strategies were same for both PV and WECS, which is explained in the latter section of the paper. Three-phase grid-connected PWM VSI PV system shown in Fig.8



(a)



(b)

Fig. 7 (a) Principle of P&O MPPT strategy (b).Flowchart of the MPPT control.

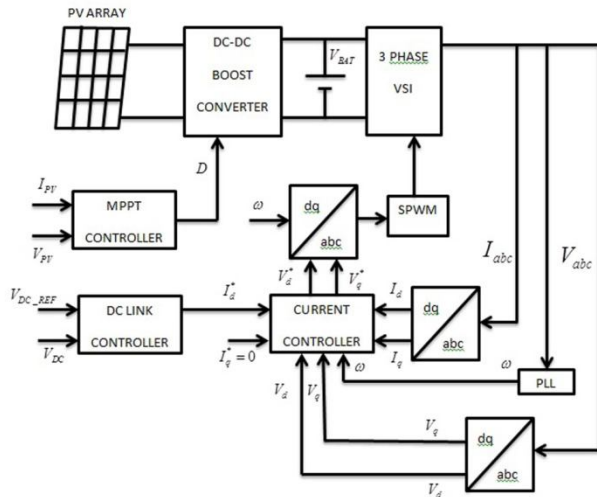


Fig.8. Configuration of grid connected solar system.

IV. MPPT CONTROL ALGORITHM OF THE WIND ENERGY SYSTEM

A. Optimum Tip speed ratio control

In the TSR control method presented in this paper, wind speed is measured for obtaining optimum rotor speed using the value of optimum tip speed ratio. The optimum TSR is obtained from the turbine's $C_p-\lambda$ curve. The rotor speed required for implementing speed feed-back control is either estimated using a speed observer or measured using speed sensor. The speed control is exercised using a PI controller. The measured speed, and further, using optimal TSR, the optimal rotor speed command is computed. The generated optimal speed command is applied to the speed control loop of the WECS control system. The PI controller controls the actual rotor speed to the desired value by varying the switching ratio of the PWM inverter. The control target of the inverter is the output power delivered to the load. This WECS uses the power converter configuration shown in Fig. 9. The block diagram of the PI-based MPPT controller module is shown in Fig. 10.

Here, the optimum speed command was generated by the MPPT controller for speed control loop of machine side converter control system enabling the WECS to extract optimum energy.

B. Design of the PI Controller

The PI controller is used in Fig. 11. The desired step command tracking response for high performance applications usually are: 1) no steady-state error; and 2) preset rising time. In addition to these two criteria, this research will further suppress the overshoot. Using the nominal plant model, the transfer function of the power response to the command input in Fig. 11 can be expressed by

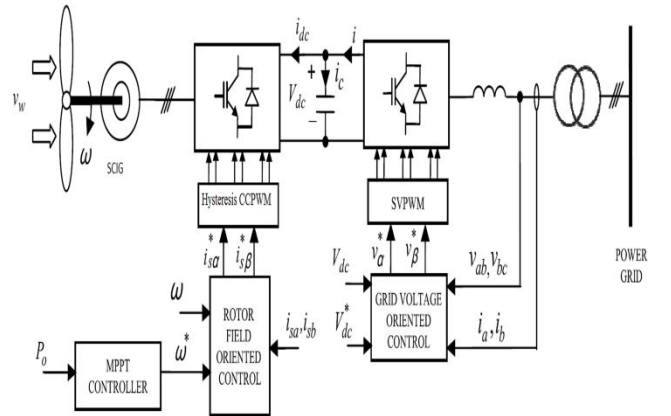


Fig.9. Configuration of wind power generation system

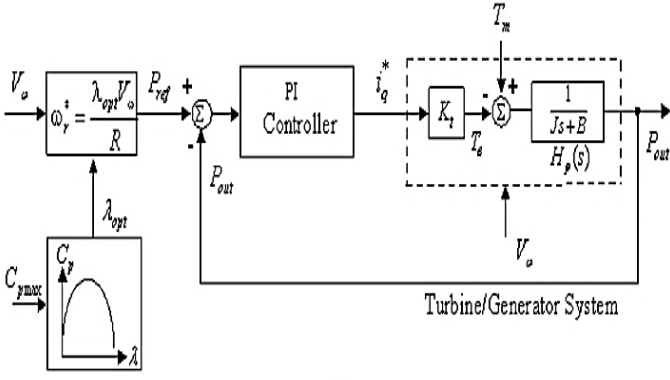


Fig.10.Wind energy control system using PI for MPPT controller.

$$\left. \frac{P_{out}(s)}{P_{ref}(s)} \right|_{T_m(s)=0} = \frac{K_I K_t}{Js^2 + (B + K_p K_t)s + K_I K_t}$$

$$\triangleq \frac{\omega_n^2}{s^2 + 2\zeta\omega_n s + \omega_n^2} \quad (6)$$

where

$$\zeta = \frac{(B + K_p K_t)}{2(JK_I K_t)^{1/2}}, \quad \omega_n = \left(\frac{K_I K_t}{J} \right)^{1/2} \quad (7)$$

With the absence of zeros, the overshoot of the step response in (6) can be avoided by setting the damping ratio $\zeta = 1$. If the unknown parameter ω_n is solved according to the prescribed specifications, the parameters of the PI controller can be computed using

$$K_I = \frac{J\omega_n^2}{K_t}, \quad K_p = \frac{(2J\omega_n - B)}{K_t} \quad (8)$$

Equation (6) also indicates that the tracking steady-state error is zero. It follows from the previous analysis that the desired tracking specifications can be completely achieved by using the simple PI controller.

V. DC LINK AND VSC CONTROL

The VSC control scheme in the double processed, three-phase, grid-connected PV and wind systems shown in Fig. 9 and Fig.10 implements regulations of DC bus voltage and unity power factor. Fig. 11 shows the block diagram of the VSC control scheme that was used in this work. The measured feedback currents i_a, i_b, i_c from the utility grid at a point of common coupling (PCC) are converted to the rotating dq reference frame oriented with the grid voltage v_a, v_b, v_c . The transformation process is known as Park transformation, which uses the following equation:

$$v_d = \frac{2}{3} \left[v_a \sin \theta + v_b \sin \left(\theta - \frac{2\pi}{3} \right) + v_c \sin \left(\theta + \frac{2\pi}{3} \right) \right]$$

$$v_d = \frac{2}{3} \left[v_a \cos \theta + v_b \cos \left(\theta - \frac{2\pi}{3} \right) + v_c \cos \left(\theta + \frac{2\pi}{3} \right) \right], \quad (9)$$

$$i_d = \frac{2}{3} \left[i_a \sin \theta + i_b \sin \left(\theta - \frac{2\pi}{3} \right) + i_c \sin \left(\theta + \frac{2\pi}{3} \right) \right]$$

$$i_d = \frac{2}{3} \left[i_a \cos \theta + i_b \cos \left(\theta - \frac{2\pi}{3} \right) + i_c \cos \left(\theta + \frac{2\pi}{3} \right) \right]$$

where the grid angle θ is obtained via a phase locked loop (PLL). The v_d, v_q, i_d , and i_q are DC variables, which can be properly controlled with a proportional integral (PI) controller.

The DC link voltage error $V_{dc} - V_{dc_ref}$ is controlled with a PI controller, which eliminates the steady-state voltage variations at the DC bus by forcing a small active power exchange with the electric grid. This process provides d-axis current reference i_{d_ref} , which is proportional to the active power that controls power flow from or to the DC side. The q-axis current component i_q is proportional to reactive power, whose reference i_{q_ref} is set to zero to maintain unity power factor.

The voltage outputs v'_d, v'_q of the current controller are converted to three modulating signals v'_a, v'_b and v'_c , using the following transformation, which is the reverse of the Park transformation:

$$v'_a = v'_d \sin \theta + v'_q \cos \theta + \frac{v_a + v_b + v_c}{3}$$

$$v'_b = v'_d \sin \left(\theta - \frac{2\pi}{3} \right) + v'_q \cos \left(\theta - \frac{2\pi}{3} \right) + \frac{v_a + v_b + v_c}{3}. \quad (10)$$

$$v'_c = v'_d \sin \left(\theta + \frac{2\pi}{3} \right) + v'_q \cos \left(\theta + \frac{2\pi}{3} \right) + \frac{v_a + v_b + v_c}{3}$$

These transformations are then used by the three-phase, VSC PWM generator to achieve the control pulses of IGBTs. The same procedure is applied to WECS Grid connected converter control.

The harmonic currents pose one big challenge to the measurement of power quality, the total harmonic distortion (THD) of the voltage, calculated according to (11):

$$THD = \left[\sum_{h=2}^{40} (u_h)^2 \right]^{1/2} \quad (11)$$

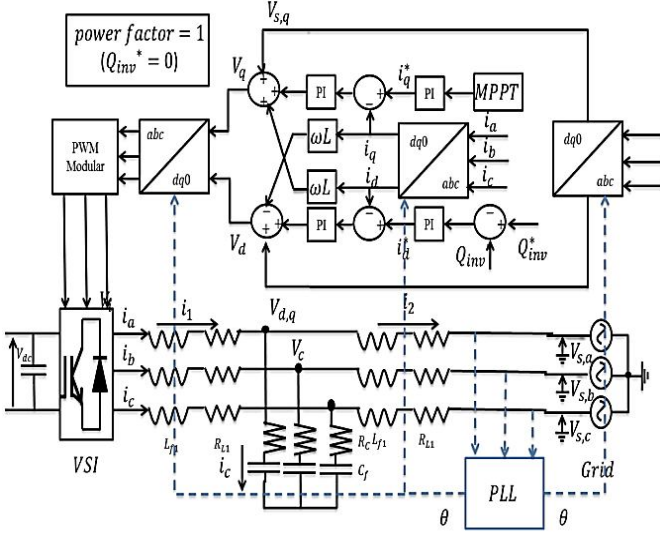


Fig.11. control strategy of a constant DC link and three-Phase VSI

Where harmonic voltages is $u_{h,s}$ and h denotes the harmonic order.

VI. RESULTS AND DISCUSSION

The proposed hybrid system was implemented in the MATLAB/Simulink environment as shown in Fig.1. Parameters of the WECS, the diesel generator, and the PV system used in the simulation are shown in Table I. Many tests were conducted to show performance of the model under various conditions, with the conventional MPPT techniques, such as typical TSR control and P & O method. Solar and Wind power systems are operated as base load plant and diesel will work as peak load plant. The simulation is run on 10 secs.

The entire simulation can be divided into three sections:

- MPPT System Performance with constant load (0-5.5secs).
- MPPT with Load Change (5.5-10 secs).
- MPPT under Variable Conditions.

A. MPPT SYSTEM PERFORMANCE

1. Wind Power MPPT

Time domain simulation was run for the hybrid power system with varying load under sufficient wind and irradiance. The output power from WECS is shown in Fig. 12, it can be seen that the PI with less transient and smaller vibrations. The average power available is 5.1 kW.

TABLE.1
SIMULATION PARAMETERS

Wind Induction Generator	
Rated Power (kW)	7.5
Voltage (V)	380
Frequency (Hz)	50
Inertia	0.7065
No. Of Pole Pairs	2
Wind Speed (m/s)	8-12
Diesel Synchronous Generator	
Rated Power (kW)	16
Voltage (V)	380
Frequency (Hz)	50
Inertia	0.8
No. Of Pole Pairs	2
PV Array	
Maximum Power of Module Unit (W)	230W@25°C,1KW/m ²
Module Number	6×4=24
Total Power Rating (kW)	0.23×24=5.52
Unit Rated Voltage (V)	30
Unit Rated Current (A)	7.8
Irradiance Level (W/m ²)	800-1000
Battery Energy Storage System	
Rated Voltage (V)	540
Capacity (kWh)	100
Load	
Capacity (kW)	9-15
Grid	
Voltage (V)	415
Frequency (Hz)	50
Phase	3

The SCIG reaches its rated speed at 1.5sec, until then the load feeds on the battery. The rotor speed will adjust corresponding to the changes in the wind speed as shown in Fig.12. This shows the better performance of the MPPT controller.

The effect of variation of wind speed is also considered along with load changes in order to show stability of the system. The wind speed falls from 12m/s to 8m/s at interval between 3-5.5secs.

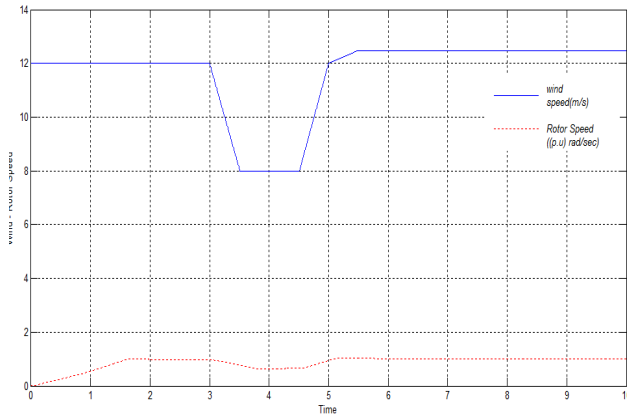


Fig.12 MPPT Tracking response of WECS.

2. Solar Power MPPT

The output power from PV is shown in Fig.13. We can see that the P&O controller provides a better performance, both in the transient and the steady state. The average power is 4.4 kW.

Here the ramp up/down signal is given as irradiance, which is varied rapidly from 1000-800-1000 at time interval between 1-3secs.

The P&O controller of the system can quickly and accurately track the maximum power output for solar array. The effective tracking of irradiance by the power and system voltage is shown in the Fig.14, indicates robustness of the P&O algorithm.

B. MPPT with Load Change

Fig.15 (a) and (b) shows the response of P&O and PI controllers for a sudden load change from 14 to 22 kW at 6.5sec. The dc-link voltage slightly decreases and then recovers in around 0.1 s.

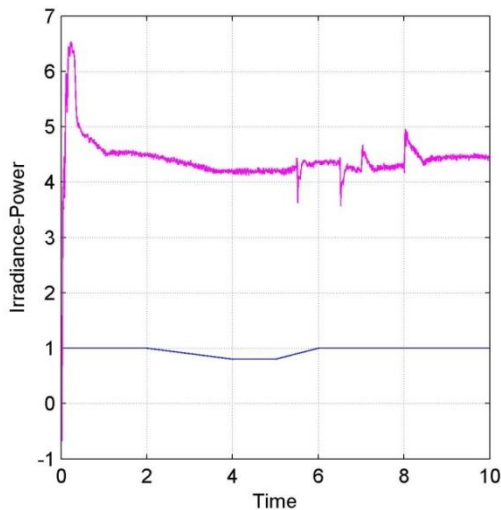


Fig.13 MPPT Tracking response of PV system.

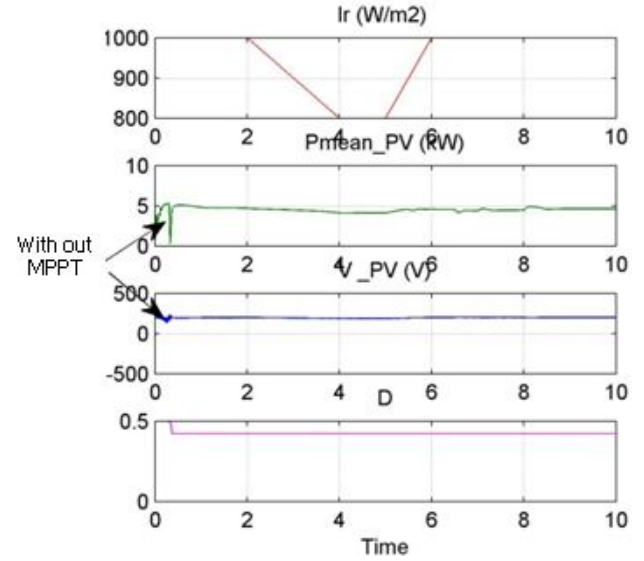
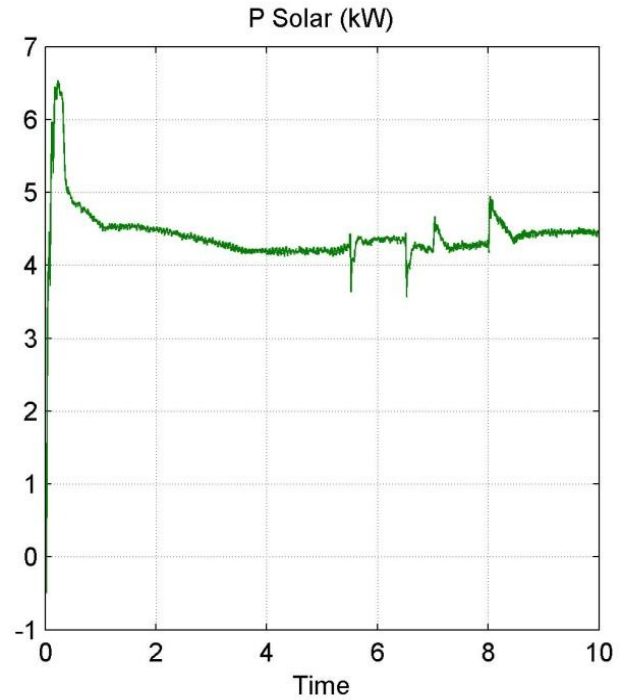


Fig.14 MPPT response by Comparing Irradiance, Power, and Voltage.

C. MPPT under Variable Conditions

This case demonstrates a changing environment, during 2 to 7 secs, the wind speed changed from 12 to 8m/s and again from 8 to 13 m/s in the time period of 3 to 5.5 secs. The irradiance level changed from 1000 to 800 W/m² and the load is changed from 8 to 22 kW.



(a)

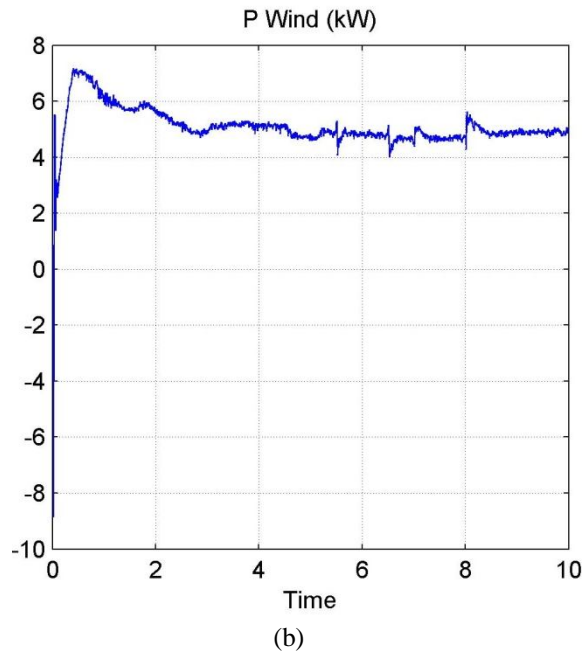


Fig. 15 MPPT response under sudden change in load for (a) Solar (b) Wind.

We can see from Fig.16 that with the drop of wind speed, the wind power also dropped to a low level around 0.2 kW. The diesel generator works with the wind turbine and PV array to meet the demand by picking up more loads. With a short transient in the beginning, the hybrid system quickly reaches stable operation. From Fig.3, the relationship between the optimal rotational speed and the power of the DGS is almost linear in this research. With normal load i.e. 8kw up to base load the mechanical input of the DGS is 0.1 With increase in load i.e., 14-kW load, the optimal speed, mechanical input of the DGS is 0.6 p.u, i.e., 43% rated speed. With 20-kW load, the control strategy drives the generator to a new optimum speed; mechanical input of DGS is 1.1p.u, i.e., 51% rated speed. The fuel savings at these reduced speeds are around 19% and 11% in comparison with the rated speed, respectively, Prime-mover input, field excitation, terminal Voltage, Speed are shown in Fig.17.

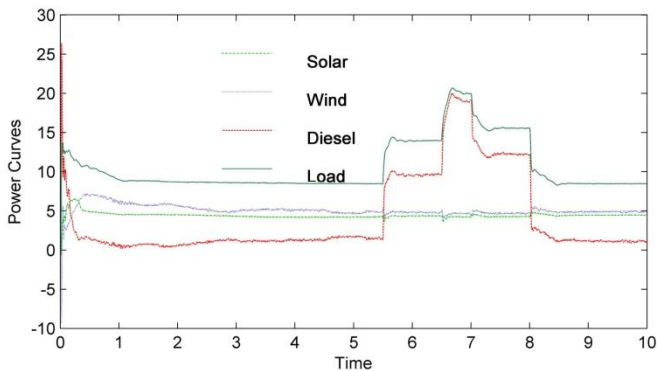


Fig.16 MPPT tracking under sudden Change in load from 5.5 to 8 secs.

Synchronous Generator will regulate the frequency of the grid, under minimum load or No-load on the utility; solar, wind and BESS would feed the load, in that condition synchronous generator will act as synchronous condenser delivering leading power factor

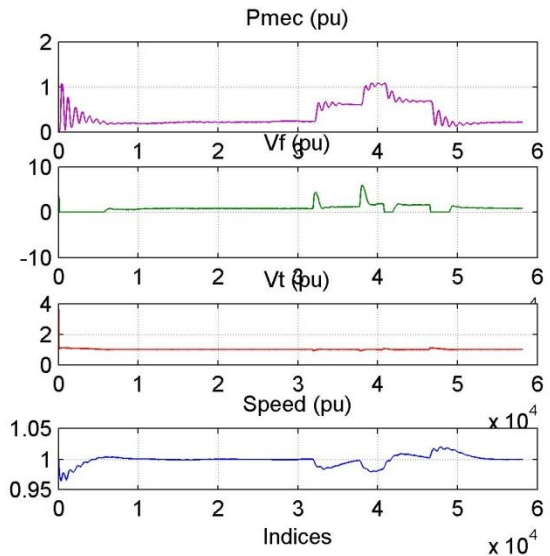


Fig.17 Governor and excitation response for sudden change in load.

The grid frequency response will not change as can be seen in Fig. 18. The proposed method can track faster with a more stable output power under load disturbance. The harmonic distortions present in the load current and voltage waveforms were observed and calculated through FFT analysis tool in Powergui in Matlab/Simulink. FFT Analysis of Grid Current, THD of 0.14% at 50 Hz .The results achieved were satisfactory and within the permissible limits in accordance to IEEE standards.

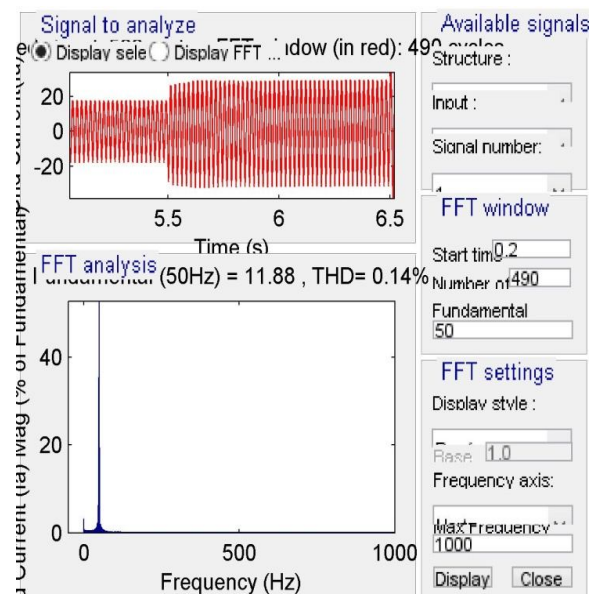


Fig.18. FFT Analysis of Grid Current, THD of 0.14% at 50 Hz

VII. CONCLUSION

In this paper, a solar and diesel–wind hybrid generation system was proposed and implemented. This stand-alone hybrid generation system can effectively extract the maximum power from the wind and solar energy sources. From the case studies, it shows that voltage and power can be well controlled in the hybrid system under a changing environment. An efficient power sharing technique among energy sources are successfully demonstrated with more efficiency, a better transient and more stability, even under disturbance. The simulation model of the hybrid system was developed using MATLAB/Simulink. The load frequency is regulated by the diesel generator by imposing the rotor currents with the slip frequency. The electrical torque of the WECS generator is controlled to drive the system to the rotational speed where maximum energy can be captured. Depending on the load size and the power supplied by the WECS generator, the control system regulates the DGS rotational speed to minimize the fuel consumption. The Power Quality of the system from the results obtained has been very good and right value for the money invested.

VIII. REFERENCES

- [1] G. Abad, M. A. Rodriguez, G. Iwanski, and J. Poza, "Direct power control of doubly-fed-induction-generator-based wind turbine under unbalanced grid voltage," *IEEE Trans. Power Electron.*, vol. 25, no. 2, pp. 442–452, Feb. 2010.
- [2] R. Dettmer, "Revolutionary energy—A wind/diesel generator with flywheel storage," *Inst. Electr. Eng. Rev.*, vol. 36, pp. 149–151, Apr. 1990.
- [3] Z. Chen and Y. Hu, "A hybrid generation system using variable speed wind turbines and diesel units," in *Proc. IEEE Ind. Electron. Soc. Annu. Meeting Conf.*, Nov. 2003, pp. 2729–2734.
- [4] B. S. Borowy and Z. M. Salameh, "Dynamic response to a stand-alone wind energy conversion system with battery energy storage to a wind gust," *IEEE Trans. Energy Convers.*, vol. 12, no. 1, pp. 73–78, Mar. 1997.
- [5] N. Femia, G. Petrone, G. Spagnuolo, and M. Vitelli, "Optimization of perturb and observe maximum power point tracking method," *IEEE Trans. Power Electron.*, vol. 20, no. 4, pp. 963–979, Jul. 2005.
- [6] B. Yang, Y. Zhao, and X. He, "Design and analysis of a grid-connected photovoltaic power system," *IEEE Trans. Power Electron.*, vol. 25, no. 4, pp. 992–1000, Apr. 2010.
- [7] T. Senjyu, Y. Ochi, E. Muhando, N. Urasaki and H. Sekine, "Speed and Position Sensor-less Maximum Power Point Tracking Control for Wind Generation System with Squirrel Cage Induction Generator", *IEEE* 2006.
- [8] Whei-Min Lin, Chih-Ming Hong, and Chiung-Hsing Chen, "Neural-Network-Based MPPT Control of a Stand-Alone Hybrid Power Generation System," *IEEE Trans. Power Electron.*, Vol. 26, no. 12, pp. 3571-3581, Dec. 2011.
- [9] R. Peña, R. Cárdenas, J. Proboste, J. Clare, and G. Asher, "Wind-Diesel Generation Using Doubly Fed Induction Machines", *IEEE Trans. Energy Convers.*, Vol. 23, no. 1, pp. 202-214, Mar. 2008
- [10] *IEEE Recommended Practice for Excitation System Models for Power System Stability Studies*, IEEE Power Engineering Society, IEEE Std 421.5TM-2005, Apr. 2006.
- [11] H. Tian, F. Mancilla–David, K. Ellis, E. Muljadi, P. Jenkins, "A Detailed Performance Model for Photovoltaic Systems," Journal Article, NREL/JA-5500-54601, July 2012.
- [12] P. Giroux, G. Sybille, C. Osorio, S. Chandrachood, "Grid-Connected PV Array," Demo in Mathworks.
- [13] Lalouni S., Rekioua D., "Modeling and simulation of a photovoltaic system using fuzzy logic controller" Proceedings of International Conference on Developments in eSystems Engineering, (DeSE), pp. 23-28, 2009.
- [14] Idjdarene K., Rekioua D., Rekioua T., Tounzi "A. Performance of an isolated induction generator under unbalanced loads", *IEEE Transactions on Energy Conversion*, vol. 25, no. 2, pp. 303-311.
- [15] Rekioua, Djamilia, Matagne, Ernest, Optimization of photovoltaic power systems: Modelization, Simulation and Control. Green Energy and Technology Series, Springer, 2012.